Chemical Engineering Journal 93 (2003) 217–224

Chemical Engineering Journal

www.elsevier.com/locate/cej

Experimental study of hydrocarbon hydrogenation and dehydrogenation reactions in silicon microfabricated reactors of two different geometries

H. Surangalikar, X. Ouyang, R.S. Besser*

Department of Chemical, Biochemical, and Materials Engineering, Chemical Engineering and Stevens Institute of Technology, Castle Point on Hudson, Hoboken, NJ 07030, USA

Received 29 July 2002; accepted 11 November 2002

Abstract

Miniaturization is fast gaining importance and relevance in chemical processes that are conventionally carried out on a lab-scale or larger. Miniaturized chemical-reaction systems, or microreactors, are devices that behave as continuous flow systems and whose dimensions are in sub-millimeter range. Microreactors were successfully fabricated using wet silicon bulk micromachining and deep reactive ion etching (DRIE) techniques, were used to characterize reactions involving heterogeneous catalysis, and demonstrated their feasibility as efficient tools in catalyst and process development. In this study, the relatively simple reactions of cyclohexene hydrogenation and de-hydrogenation over a platinum catalyst were studied, reactions which are models for important classes of reactions of significance in petroleum industry. The conversion, selectivity and yield for products cyclohexane and benzene, were measured as a function of temperature and reactant flow rates. The experiments were done in microreactors of characteristic dimensions of 100 and 5 μm. The results are shown which compare the performance of these two types of reactors.

Keywords: MEMS; Miniaturization; Cyclohexene; Dehydrogenation; Petroleum; Catalysis; Selectivity; Conversion; Mass transport

1. Introduction

The developments in the area of chemical process miniaturization have taken large strides in the past few decades due to the evolution of silicon micromachining techniques (bulk and surface), which make the generation of devices with sub-millimeter and sub-micrometer dimensions possible. These developments gave rise to ideas like chemical laboratory on chips (LOC) and micro-electro-mechanical systems (MEMS). The LOCs can be perceived as complete systems integrated on a single substrate capable of analyzing and synthesizing chemicals [1]. Chemical reaction microsystems, or microreactors, can be integrated with other devices like pressure transducers, flow controllers and temperature control apparatus to form complete systems capable of analyzing or synthesizing chemicals [2]. Microreactors, owing to their small dimensions have many advantages over the conventional lab-sized reactors because they consume less space, materials, and energy and have shorter response times. Thus, as lab-reactors, they are more efficient than the latter because of more information gained per unit time and space [3]. Microreactors are continuous microfluidic systems having characteristic dimension of the order of 1–1000 μm, exceedingly low volumes of reaction, and high aspect ratios, allowing the application of high temperature and concentration gradients to study reactions in extreme temperature and/or pressure regimes with little or no danger of explosion [3,4]. Laminar flow in microreactor channels is another advantage as this flow is more energy efficient than turbulent flow and allows for closer process control and better performance [5]. They also produce negligible chemical waste, allow easy integration with other devices, and easy control of reaction parameters due to small volume. These inherent advantages make microreactors very important in fields of chemistry, molecular biology, pharmaceuticals and chemical engineering. Microreactors can be used in process development where it is logical and economic to simulate a reaction on a small scale to make kinetic studies and then use the relevant data to design large-scale processes [3].

Microreactors offer great potential when used in large numbers for on-site and on demand synthesis of chemicals and also for studies in heterogeneous catalysis for rapid catalyst evaluation and development [2,6]. Microreactors have

* Corresponding author. Tel.: +1-201-216-5257; fax: +1-240-255-4028.
E-mail address: rbesser@stevens-tech.edu (R.S. Besser).

1385-8947/02/$ – see front matter
doi:10.1016/S1385-8947(02)00339-X

better heat and mass transfer properties and uniform flow and temperature distributions without any dead zones and have fast response times due to low volume. Thus, they are ideal for parallel processing for high throughput testing where different reactions can proceed in an array of microreactors without any interference by flow mixing, thus ensuring high accuracy and reliability of the data and high speeds of analysis [3].

The reactions under consideration in this study are the hydrogenation and dehydrogenation of cyclohexene, over a Pt catalyst, which are model reactions for important reaction classes in petroleum industry [7]. Reactions were successfully studied for conversion, selectivity and yield by varying the operating conditions of flow rates of reactants and the reaction temperature. The following reactions were carried out in two different reactor geometries, with characteristic dimensions of 100 and 5 μm.

$$C_6H_{10} + H_2 \rightarrow C_6H_{12} \quad (1)$$

$$C_6H_{10} \rightarrow C_6E_6 + 2H_2 \quad (2)$$

In all cases, channel depth was 100 μm and length was 1.8 cm.

The results show that these microreactors can be characterized for a variety of reactions to acquire valuable data on reaction kinetics and catalyst deactivation and reactivation in a safe and economical way. This, coupled with fast response times, ease of operation and reproducibility, shows the feasibility of microreactors as versatile laboratory tools for the testing and development of new catalyst systems.

2. Microreactor fabrication

The microreactors, comprising of channels etched in a silicon substrate were fabricated using the well-known silicon bulk micromachining techniques involving photolithography and etching [8,9]. The starting material for microreactor fabrication was a (1 1 0)-silicon wafer coated with SiO_2 (which acts as the etching mask layer) on both sides. The desired geometry can be developed in the silicon substrate by creating a pattern in the photoresist and then transferring this pattern to the SiO_2 layer below it by buffered oxide (HF) etching. The removed SiO_2 then allows the silicon in that area to be etched by KOH solution to obtain the desired channel geometry in the bulk of the silicon. As KOH is an anisotropic (unidirectional) etchant, and has a high etching rate for silicon in a (1 1 0) wafer, it is possible to create flat vertical structures or channel walls in the silicon substrate with high aspect ratios. These channels then form the reaction zone of the microreactor. The same procedure is repeated to form vias on the front side and the backside of the channel, which form the inlet and outlet for the gaseous species involved in the reaction. The first kind of microreactor has channel width of 100 μm and 39 channels in the reaction zone. The second kind has channel width of 5 μm and 780 channels in the reaction zone, and these were fabricated using ICP etching, which is a kind of deep reactive ion etching and uses a reactive gas, SF_6, as an etching medium.

After formation of the reactor structures, chips were separated from the wafer and catalyst was deposited in the microchannels. Vacuum sputtering was used to selectively deposit a thin film of Pt (10–40 nm) within the channels and the top of the channel separation walls. A shadow mask was incorporated during the deposition to prevent the periphery of the top surface from receiving deposition. The final film is flat and featureless when viewed by scanning electron microscopy, and yields no surface area enhancement. As such, film thickness variations, which are expected to exist along the channel depth, are inconsequential. Surface coverage was found to be complete, yielding a catalyst surface area of approximately 2 cm^2 for the 100 μm devices, and 28 cm^2 for the 5 μm devices. Finally, the microreactors were anodically bonded with Pyrex glass to form robust, airtight devices, as shown in Fig. 1.

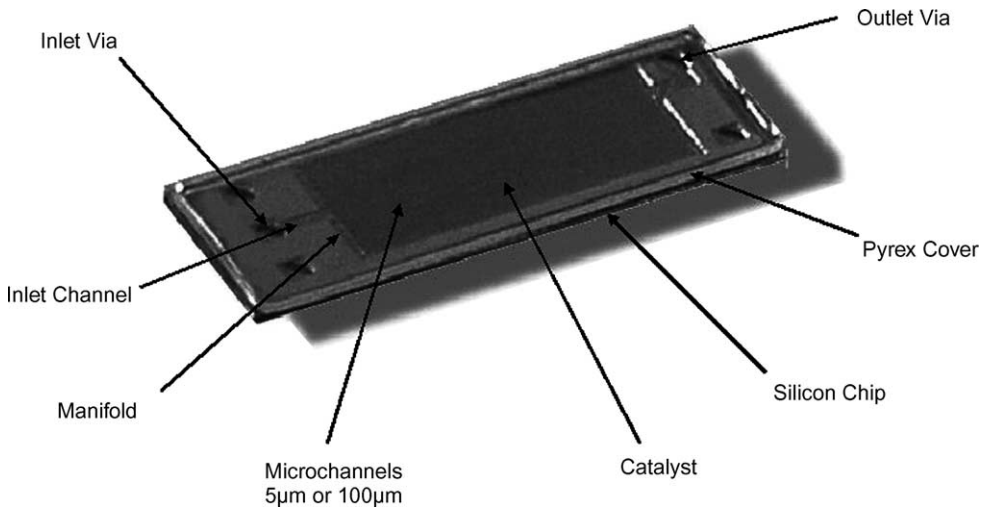

Fig. 1. A completed microreactor device 1 cm × 3 cm in size.

3. Microreactor characterization

These microreactors were characterized in an experimental setup that allows the reacting gases to pass through the reactor and the effluents to be analyzed by a mass spectrometer. The setup is comprised of three parts: (a) a mounting-heating block, integrated with an air-tight tubing system, including mass flow controllers, pressure transducers, and a vacuum pump, (b) a data acquisition interface between the setup and a computer using LabVIEW software for computerized control of temperature, gas flows, and pressure, and (c) a quadrupole mass spectrometer (QMS), for qualitative and quantitative analysis of the reaction products [10,11].

The microreactors were mounted on a specially made heating block, which has the inlet and outlet connections to the rest of the tubing system. The inlet and outlet vias of the microreactor were connected to the corresponding holes in the block and compression-sealed using O-rings. The inlet and outlet of the heating block were connected to the outer 1/16 in. (1.59 mm)-diameter stainless steel tubing with the help of Swagelok fittings. External mass flow controllers monitored the flow of the reactant hydrogen, from the cylinder. As the other reactant, cyclohexene, is liquid under ambient conditions, argon gas was bubbled into the cyclohexene reservoir, so that argon saturated with cyclohexene (C_6H_{10}) vapor forms the other feed gas to the microreactor. The reactor temperature was controlled with the help of solid-state-relay driven resistive heating cartridges and a thermocouple. Temperature uniformity was checked manually with a thermocouple contact probe and found to be better than 5 °C. Temperature was controlled based on a single measurement of the support block in close proximity to the reactor. The data acquisition software interface allowed the recording of instantaneous values of temperature, flows, and pressures.

The microreactor effluents were continuously sampled by the QMS, which measured the partial pressures of all the species present in the effluent stream. Since very low flow rates were involved in the experiments, the effluent stream was diluted with He gas to ensure a minimum required flow rate of the effluent sample for the QMS, and at the same time to prevent the pumping system in the QMS from adversely affecting the operating pressure in the reactor. He was used rather than Ar (the carrier for the cyclohexene) so that the individual flow rates of these streams could be separately accounted for. Since the QMS was originally calibrated only for ambient air, all the species involved in the reaction were individually calibrated and their respective sensitivity factors determined. Analysis was done by measuring the partial pressure continuously over a pre-specified mass range (analog or a histogram scan), or for desired mass numbers only. For example, in these experiments, the monitored quantities were the atomic mass units (AMU) of the reactants, cyclohexene (80) and hydrogen (2), and the products cyclohexane (84) and benzene (78), along with the carrier gas argon (40) and dilution gas helium (4). The variation of partial pressures at each of these masses is recorded as partial pressures versus time (P versus t) scan for the entire length of the experiment, as shown in Fig. 2.

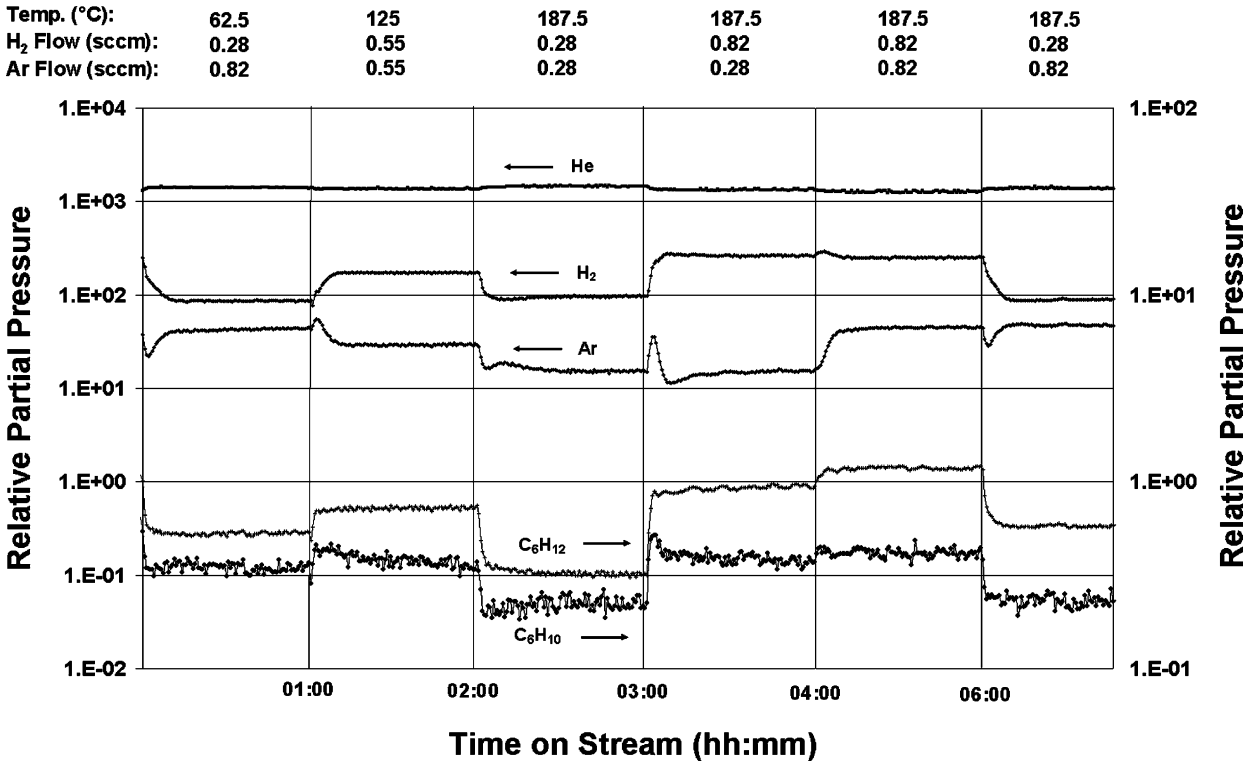

Fig. 2. A sample P vs. t scan, showing the change in partial pressures of the reactant and product species.

4. Experimental

A number of microreactors (named *E* through *H*, where $E = 100\,\mu m$, $F = 100\,\mu m$, and $H = 100\,\mu m$, and $G = 5\,\mu m$) were used in the study. Each microreactor was mounted on the heating/mounting block and was positioned precisely on the O-rings to make an airtight seal for the reactor. The seal was checked by evacuating the tubing system and then isolating it to observe a steady level of vacuum. The tubing system was then evacuated for a period of 1 h to remove any traces of gaseous impurities so that a standard background could be established in the QMS before the start of the actual reaction. H_2 gas was allowed to flow through the reactor for an hour at room temperature as a method of pre-treatment of the Pt catalyst. The Ar/C_6H_{10} stream was introduced into the system to register a pure background level for the reactant. Once the partial pressure was steady, the H_2 flow was introduced and the temperature elevated to the desired value. The partial pressures of all the involved species were monitored throughout the length of the experiment by the *P* versus *t* scan. In addition, a stability test, to account for the sensitivity of the mass spectrometer over time and usage, was performed by recording the strength of the Argon signal at the start of each experiment.

5. Determination of rate-limiting step in the microreactor

A reaction in heterogeneous catalysis proceeds in a combination of elementary steps like mass transport of the reactants from the bulk of the fluid to the catalyst surface, adsorption, surface reaction on the catalyst, and desorption of the products from the catalyst surface. Each of these steps has its own rate that depends upon the conditions of temperature and pressure, and hence, the step that has the lowest rate has the greatest influence on the overall rate of reaction [12]. This step is designated as the rate-limiting or rate-controlling step and its determination is important so that necessary measures can be taken to account for, and hopefully minimize its effect on the overall rate of the reaction.

For the reactions under consideration in this study, a comparison was made between the rate of mass transport of the cyclohexene molecules from the bulk of the gas phase to the catalyst surface, and the rate of reaction at the catalyst surface, so as to be able to identify the regime in which the microreactor operates, namely mass-transport-limited or reaction-rate-limited. The rate of mass transfer is calculated from mass transfer coefficient (MTC), which is analogous to heat transfer coefficient [12,13]. It is well-known that an analogy can be drawn between heat and mass transfer for similar geometries, and the relations for heat transfer be used in mass transfer coefficient calculations by replacing the Nusselt number (*Nu*) by the Sherwood number (*Sh*) and the Prandtl number (*Pr*) by the Schmidt number (*Sc*) [13]. Calculations of the Reynolds number and entry length show that the flow in the microreactor was a fully developed laminar flow as expected, due to small hydraulic diameter and low flow rates. For this condition, the value for the Nusselt number in the case of convective heat transfer in a circular tube is known to be approximately 4 [13], which was directly used as the Sherwood number as defined by the analogy. The Sherwood number is mathematically represented as

$$Sh = \frac{K_c \times D_h}{D_{ab}} \tag{3}$$

where K_c is the MTC, D_h the hydraulic diameter for the channel section, and D_{ab} is the diffusivity of C_6H_{10} in the gas mixture, calculated on the basis of mole fractions of the gas species in the mixture [14]. From this relation, the value of K_c can be estimated and used to calculate the molar flux of C_6H_{10} molecules by the relation:

$$J_a\,(\text{kmol/m}^2\,\text{s}) = K_c\,(\text{m/s}) \times (C_a - C_{as})\,(\text{kmol/m}^3) \tag{4}$$

where C_a and C_{as} are the molar concentrations of C_6H_{10} in bulk and at the surface respectively. For the purposes of calculations, a worst case maximum for the mass transfer rate is desired, $C_a - C_{as} \approx C_a$ is taken, and hence,

$$J_{a,max} = K_c \times C_a \tag{5}$$

This value of $J_{a,max}$, which is the rate of mass transport of C_6H_{10} molecules to the catalyst surface, was then compared to the rate of the reaction occurring on the catalyst surface, $-r_a$ (kmol/m^2 s), which was calculated from conversion and selectivity data, and is a measure of the rate of consumption of C_6H_{10} molecules at the catalyst surface.

The above calculations for $J_{a,max}$ and $-r_a$ were done at given values of reactant flow rates, H_2 and Ar/C_6H_{10}, temperature and pressure. Calculations performed on the 100 and 5 μm chips show that the values for molar flux, $J_{a,max}$ are about three orders of magnitude higher than the values for $-r_a$. Thus, the rate of consumption of C_6H_{10} molecules in the surface reaction is inherently slower than the rate of mass transfer of C_6H_{10} molecules from the bulk of the gas to the surface. Thus, it can be safely concluded that the microreactors operate in a reaction-limited mode and that the surface reaction is the rate-limiting step. This analysis agrees with the result of a model that was created and reported upon earlier for the 100 μm reactor [15]. This model, based only on the surface reaction rate and assuming negligible mass transfer rates, closely matched the conversion versus temperature behavior of the reactor, implying that the surface reaction rate is limiting.

It is important to note here that most industrial reactions are carried out in mass-transfer-limited mode, where the rates of adsorption and desorption of the reactants and products depend on conditions of temperature, pressure and fluid velocities employed [16]. If the fluid velocities employed are not sufficiently high, the rate of mass transfer to the surface, for example in reactors operating at atmospheric pressures

or higher, would be very slow, giving rise to an added resistance to the progress of the reaction to completion. Thus, high fluid velocities, and hence, turbulent conditions, have to be employed for most industrial reactions to favor faster mass transfer. This problem can be better addressed with the help of microreactors, as the calculations on the operation of the microreactors show that the rates of mass transfer are sufficiently higher than the rate of reaction on the catalyst surface even in laminar conditions, which in comparison to turbulent conditions make the process more energy efficient, easier to simulate, and allow for better process control and higher yields [5].

6. Results and discussion

6.1. Effect of variation in flow composition

The experiments performed were aimed at measuring the basic parameters of a chemical reaction like conversion, selectivity and yield at varying flow rates of the reactants and reaction temperature, and also to compare the performance of 100 and 5 μm reactors under these conditions. Flow variation followed the systematic settings of Table 1 whereby one reactant stream flow was held constant and the other stream cycled through the values shown. Next, the first reactant flow was set to a new value, the process repeated, etc. Partial pressure data from the mass spectrometer confirmed the production of both cyclohexane and benzene, depending upon the operating conditions of reactant flows, temperature and time on stream. Let it be noted that all plots discussed later, except where specifically designated, reflect operation of the reactor at a temperature of 200 °C and atmospheric pressure, after a time on stream of short enough duration that catalyst activity was within approximately 10% of its initial value. These settings were chosen because the system displays interesting reforming, i.e. hydrogen producing, behavior under these conditions, despite progressively decreasing activity as discussed in the following sections.

Fig. 3 shows the effect of mean residence time on the reaction conversion. The mean residence time is a function of the reactant flow rates and reactor temperature employed at that time. The conversion was found to be a strong function of residence time in 100 μm chips where it changed from about 15% at a minimum to about 80% maximum. But in 5 μm chips the change in conversion was small, which is due to the fact that 5 μm chips have an increased surface area, which accommodates the increase in flow rate, and hence, the decrease in residence time does not bring about a large change in conversion. On the contrary, in 100 μm chips, the conversion at low residence times (or higher flow rates) drops, as these have a smaller surface area (by a factor of 14) than 5 μm chip, and the incoming C_6H_{10} molecules are more likely to go un-reacted due to the slow rate of reaction on the catalyst surface.

Table 1
Reactant flow variations used in experiments

H_2 (standard cm^3/min)	Ar/C_6H_9 (standard cm^3/min)
0.1	0.3
0.3	0.6
1.0	1.0

One of the reactants was held constant while the other reactant was varied over the values shown. The first reactant was then reset to a new value and the process repeated, etc.

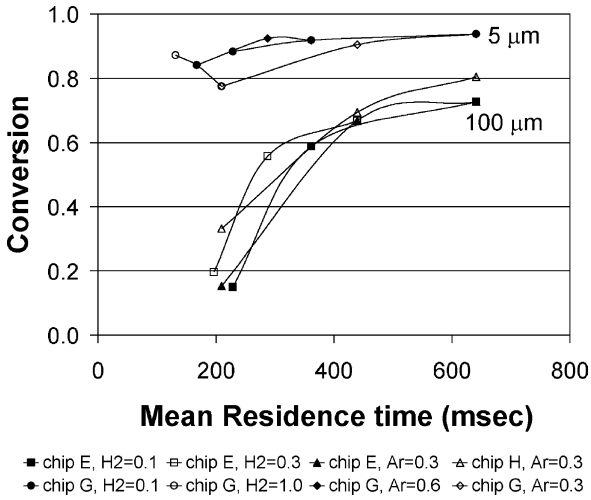

Fig. 3. Effect of mean residence time on conversion at 200 °C and 1.01 bar. All flows in standard cm^3/min.

Fig. 4 displays the effect of reactant feed ratio, as a partial pressure ratio, $P_{H_2}/P_{C_6H_{10}}$, on conversion behavior. For both 5 and 100 μm cases, the conversion follows an upward slope at low $P_{H_2}/P_{C_6H_{10}}$, and a downward slope at

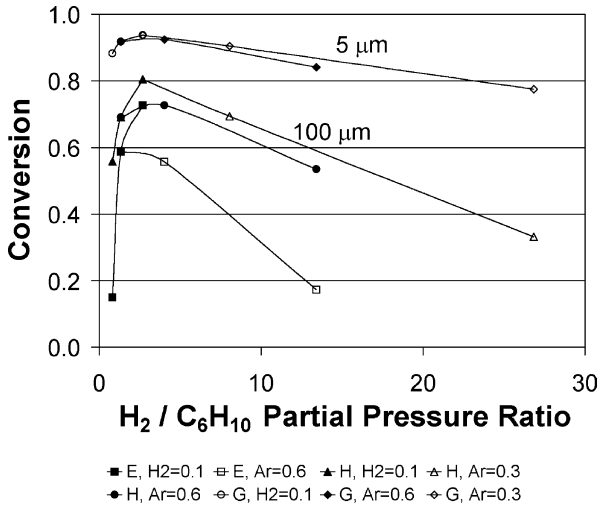

Fig. 4. Effect of reactant partial pressure ratio partial pressure on conversion at 200 °C and 1.01 bar. The legend designates the chip under test (*E*, *H*, or *G*) and which flow was held constant (H_2 or Ar/C_6H_9). The other flow was varied according to Table 1. All flows in standard cm^3/min.

high $P_{H_2}/P_{C_6H_{10}}$. In the 5 μm case, however, these slopes are much less, and the overall variation of conversion is far smaller than for 100 μm. As will be made evident in the following discussion on selectivity, the increasing slope of conversion at low $P_{H_2}/P_{C_6H_{10}}$ occurs in a regime heavily dominated by benzene production. Increasing P_{H_2} increases the rate of cyclohexane production by reaction dynamics in accord with Eq. (1), but there is a concomitant decrease of benzene production. Therefore, production rates of both species must increase in this regime in order to net a growing rate of conversion. While the increase in cyclohexane production is logical with increasing H_2 concentration, it is counter intuitive that benzene production should increase under these conditions given that H_2 should force the dehydrogenation reaction in the opposite direction. However, it is known that H_2 must be present to effectively condition metallic Pt catalysts for dehydrogenation [7,17]. In fact we have observed in the experimental system described here that dehydrogenation of C_6H_{10} cannot be made to occur without H_2 flow. Hence, below some threshold, like that observed in Fig. 4, increasing the H_2 concentration produces more favorable catalytic conditions for dehydrogenation as well as hydrogenation leading to a greater net rate of conversion of C_6H_{10}.

The region of the decreasing slope of conversion at higher $P_{H_2}/P_{C_6H_{10}}$ corresponds to conditions created by increasing the H_2 flow rate, and hence, reducing the mean residence time. Thus, the effect of decreasing conversion on the right portion of Fig. 4 can be attributed to decreasing residence time, which effect was demonstrated in Fig. 3 as being strong for 100 μm and weak for 5 μm as in the present figure.

The selectivity to the products cyclohexane (C_6H_{12}) and benzene (C_6H_6) also strongly depends on the partial pressure of the reactant species, cyclohexene and H_2. Fig. 5 shows the dependence of selectivity to C_6H_{12} and C_6H_6 on the reactant feed ratio. At a given Ar/C_6H_{10} flow, the ratio $P_{H_2}/P_{C_6H_{10}}$ is increased by increasing the H_2 flow and as the H_2 flow is increased, the reaction direction in Eq. (2) shifts towards the reactant C_6H_{10} and less of benzene is formed, whereas, the increase in H_2 favors the reaction in Eq. (1), and hence, selectivity to C_6H_{12} increases. At a given H_2 flow, reducing the Ar/C_6H_{10} flow increases the ratio $P_{H_2}/P_{C_6H_{10}}$ and as the C_6H_{10} is reduced, the H_2 becomes relatively more abundant making the reaction in Eq. (1) more probable, and hence, the selectivity to C_6H_{12} goes up, except at low H_2 flow, when the decrease in C_6H_{10} will force the reaction direction towards the reactant and be more suited to form C_6H_6. Thus, the increase in $P_{H_2}/P_{C_6H_{10}}$ increases selectivity to C_6H_{12}, and decreases selectivity to C_6H_6, indicative of the fact that increase in H_2 flow helps to form C_6H_{12} and increase in Ar/C_6H_{10} flow, or decrease in H_2 flow, helps to form C_6H_6.

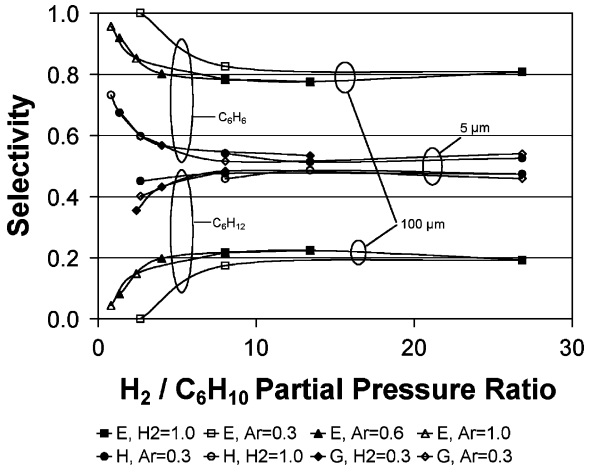

Fig. 5. Effect of reactant partial pressure ratio on selectivities at 200 °C and 1.01 bar. All flows in standard cm^3/min.

While the above discussion helps us understand the effects of varying reactant composition on conversion and product selectivity, Fig. 6 shows us the variation in C_6H_6 and C_6H_{12} selectivity with temperatures and both the 100 and 5 μm chips respond similarly to increase in reaction temperature. It is observed that at low temperatures, the reaction proceeds towards both the products initially and then the selectivity to C_6H_{12} is almost 100% when temperature reaches about 50 °C. C_6H_{12} is the more favored product as the temperature continues to rise until about 130 °C, when the selectivity to C_6H_{12} begins to drop and the selectivity to C_6H_6 rises. This shift in selectivity at higher temperatures is due to the changing catalytic surface conditions, and an effort to explain it in more detail is made later in this discussion [18,19].

The above observation is also supported by the fact that the selectivity to C_6H_6 is at a higher level than selectivity to C_6H_{12} (Fig. 5), as the measurements for these plots were made at 200 °C. Also, the selectivity to C_6H_6 in 5 μm chips is found to be at lower levels than that in 100 μm chips, explanation for which can be found in the next part of the discussion.

6.2. Discussion of reaction mechanism and shift of selectivity at higher temperatures

The results of earlier spectroscopic studies, like EELS, HREELS, IRAS, etc., on cyclohexene reactions over Pt surfaces at low pressures have revealed the presence of a C_6H_9 intermediate over the Pt surface, which then dehydrogenated to form benzene [18]. Since the above techniques are unsuitable for studies at high-pressure conditions, researchers have used a more recent and advanced technique called sum frequency generation (SFG) only to find that the intermediates in high-pressure conditions are different from those in UHV conditions [18,19]. At high pressures, the intermediates detected were 1,3-cyclohexediene (1,3-CHD) and 1,4-cyclohexediene (1,4-CHD), both of which have molecular formula C_6H_8.

It was found that the double bond in the molecular structure of the cyclohexene molecule plays an important role in forming a bond with the Pt surface, most likely by donating its π-electron density to the metal atoms to form the

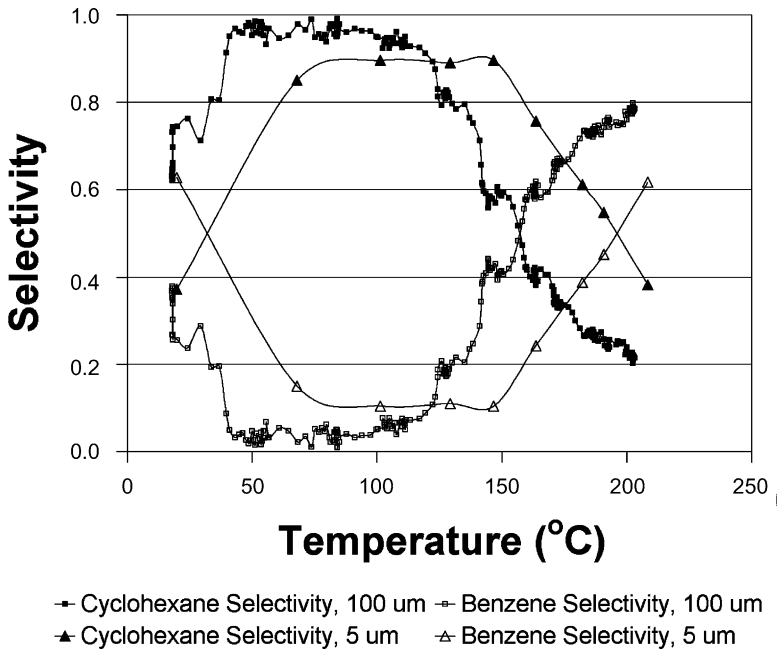

Fig. 6. Shift in product selectivity at increasing temperatures. Benzene selectivity increases at higher temperatures, as dehydrogenation becomes the favored reaction. Ar flow, 1.0 standard cm^3/min; H_2 flow, 0.3 standard cm^3/min.

intermediate species [18]. As against the earlier explanations of mechanism of this reaction that relied on a sequence of elementary steps involving interaction between H_2 and C_6H_{10} in the adsorbed state [20], this recent approach takes into account the chemical rearrangement that takes place between the C_6H_{10} molecules and the surface atoms to form the reaction intermediate species. Thus, it can be inferred that this chemical rearrangement takes a different path, forming a C_6H_9 intermediate at low pressure conditions and 1,3-CHD and 1,4-CHD at high pressure conditions.

SFG studies have shown that at near room temperatures, there is evidence of both the intermediates, 1,3-CHD and 1,4-CHD, and at temperatures above 27 to about 130 °C, 1,3-CHD is the more prominent species and the rate of hydrogenation reaction is found to be higher. This is consistent with the findings of the formation of both the products C_6H_{12} and C_6H_6 in this temperature range, selectivity being higher for C_6H_{12}. At temperatures higher than about 130 °C, the SFG studies have shown that 1,4-CHD becomes the more prominent species, and the rate of dehydrogenation is higher than the rate of hydrogenation. This is also consistent with the selectivity data, as shown in Fig. 6. It has been found that 1,3-CHD is increasingly unstable at high temperatures and tends to either dehydrogenate to C_6H_6 or change to 1,4-CHD, which ultimately forms C_6H_6, as the active surface sites now favor the dehydrogenation reaction instead of the hydrogenation reaction.

Another explanation that may be given for this change in selectivity to benzene at higher temperatures is related to the carbonaceous coverage at high pressures. At high pressures, the Pt surface is deposited with a high coverage carbonaceous layer within a short time [21], due to which sites needed for dehydrogenation are not readily available. But as the temperature increases, the adsorbed species may decompose or desorb and make the necessary sites available for dehydrogenation. This might explain the fact that the 5 μm chips, which have a surface area greater than the 100 μm chips by a factor of 14, and hence can support a larger buildup of carbonaceous layer within the reactor, show lower selectivity to C_6H_6 as compared to the 100 μm chips at a given temperature above 130 °C, and a given time on stream. As noted above, the change in selectivity is progressive and is correlated to the progressive decrease in activity. The larger surface area available in the 5 μm reactor could essentially forestall ultimate changes in these quantities longer than the smaller area 100 μm reactors for the same flow conditions.

The effect of increased surface area is also observed on the space–time–yield (STY_A) of C_6H_6, based on catalyst area, defined as the yield of product times reactant feed rate per unit surface area of catalyst. For a given flow rate of Ar/C_6H_{10}, the STY_A for C_6H_6 is greater in 100 μm chips than in 5 μm chips as shown in Fig. 7 due to the much greater catalyst loading of the 5 μm chips (by a factor of 14), a quantity which appears in the denominator of the STY_A calculation. The 100 μm chips are more productive than their 5 μm counterparts because the flow conditions are better matched to the reactor, resulting in higher productivity. However, it is expected that the 5 μm chips would continue to show increasing productivity as flow rates are

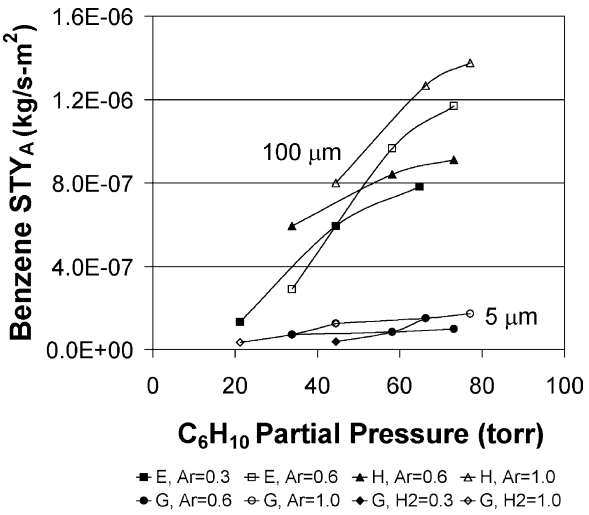

Fig. 7. Comparison of benzene space–time–yield per area (STY_A) in 100 and 5 μm reactors at 200 °C and 1.01 bar. All flows in standard cm^3/min.

raised above the highest levels tested here. This suggests further experiments for follow-on investigations.

Along with the shift in selectivity of the reaction shifts towards benzene, there is a distinct drop in conversion at higher temperatures, as observed in Fig. 8, where the conversion begins to drop at temperatures around 130 °C [21,22]. This phenomenon has been studied earlier and similar observations have shown that the catalyst activity begins to suffer at temperatures of about 130 °C and higher. This drop in conversion is likely due to progressive deactivation of the catalyst surface as the carbonaceous species is irreversibly deposited on the catalyst surface, thus blocking the sites that helped in the dehydrogenation reaction [21–23].

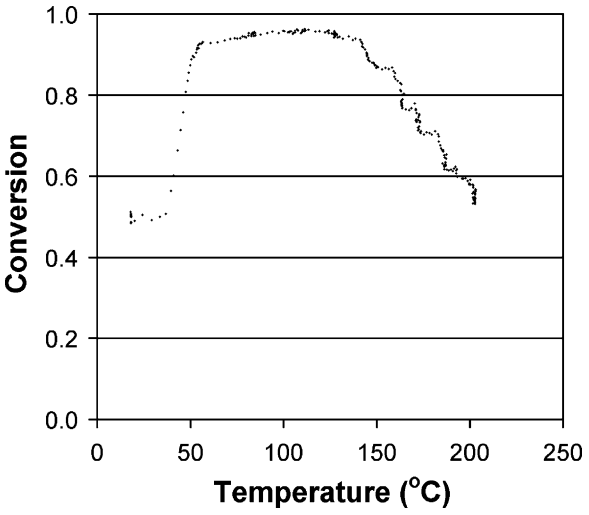

Fig. 8. Effect of increasing temperature on conversion. Depleting catalyst activity causes the conversion to drop at higher temperatures. Ar flow = 1.0 standard cm^3/min; H_2 flow = 0.3 standard cm^3/min. Temperature was held constant for 15 min at each of nine temperatures.

7. Conclusions

Conversion and selectivity studies on cyclohexene hydrogenation and dehydrogenation reactions were carried out successfully in microreactors. The flexibility of microreactors has been demonstrated with respect to reactor geometry and complex reactions as well as their feasibility in arrays, either for synthesis of chemicals on-site and on-demand, or for parallel screening of different catalyst materials for rapid development of catalyst systems. It has also been shown that the microreactors have high rates of mass transport even under laminar conditions, which is advantageous as compared to conventional reactors. Also, the conversion and selectivity data from these experiments were consistent with the findings of previous studies on these reactions.

References

[1] Lab-on-a-Chip: The Revolution in Portable Instrumentation, 2nd ed., Wiley, New York, 1997.
[2] R. Srinivasan, I.M. Hsing, P.E. Berger, K.F. Jensen, AIChE J. 43 (1997) 3059–3069.
[3] W. Ehrfeld, V. Hessel, H. Lowe, Microreactors, New Technology for Modern Chemistry, 1st ed., Springer-Verlag, Weinheim, 2000.
[4] K.F. Jensen, Technical Digest of the 2000 Solid-State Sensor and Actuator Workshop, June 2000, Hilton Head Island, South Carolina, 105-110, IEEE, Piscataway, NJ, 2000.
[5] A. Shanley, N.P. Chopey, G. Ondrey, P. Parkinson, Chem. Eng. 104 (1997) 30–34.
[6] S. Senkan, K. Krantz, S. Ozturk, V. Zengin, I. Onal, Angew Chem. Int. Ed. 38 (1999) 2794–2799.
[7] P.H. Emmet, Catalysis, vol. III, Hydrogenation and Dehydrogenation, Reinhold Publishing Corporation, New York, 1955.
[8] H. Lowe, W. Ehrfeld, Electrochim. Acta 44 (1999) 3679–3689.
[9] G.T. Kovacs, N.I. Maluf, K.E. Petersen, Proc. IEEE 86 (1998) 1536–1551.
[10] D. Lichtman, J. Vac. Sci. Tech. A 2 (1984) 200–206.
[11] P.H. Dawson, Quadrupole Mass Spectrometry and Its Applications, AIP Press, New York, 1995.
[12] H.S. Fogler, Elements of Chemical Reaction Engineering, 2nd ed., Prentice-Hall, Upper Saddle River, NJ, 1992 (Chapter 10).
[13] J.R. Welty, C.E. Wicks, R.E. Wilson, G.L. Rorrer, Fundamentals of Momentum, Heat, and Mass Transfer, 4th ed., Wiley, New York, 2001, pp. 320–322, 572–573.
[14] R.H. Perry, D. Green, Perry's Chemical Engineers' Handbook, 6th ed., McGraw-Hill, New York, 1984.
[15] R.S. Besser, X. Ouyang, H. Surangalikar, Hydrocarbon hydrogenation and dehydrogenation reactions in microfabricated catalytic reactors, Chem. Eng. Sci. 58 (2003) 19–26.
[16] J.M. Thomas, W.J. Thomas, Introduction to the Principles of Heterogeneous Catalysis, Academic Press, London, 1969.
[17] G.A. Somorjai, Introduction to Surface Chemistry and Catalysis, Wiley, New York, 1994.
[18] Su. Xingcai, K.Y. Kung, J. Lahtinen, Y. Ron Shen, G.A. Somorjai, J. Mol. Catal. A 141 (1999) 9–19.
[19] K.R. McCrea, G.A. Somorjai, J. Mol. Catal. A 163 (2000) 43–53.
[20] E.E. Gonzo, M. Boudart, J. Catal. 52 (1978) 462–471.
[21] S.M. Davis, G.A. Somorjai, J. Catal. 65 (1980) 78–83.
[22] R.K. Herz, W.D. Gillespe, E.E. Petersen, G.A. Somorjai, J. Catal. 67 (1981) 371–386.
[23] G.A. Somorjai, Carrazza, J, Ind. Eng. Chem. Fundam. 25 (1986) 63–68.